Electronic Supplementary Material (ESI) for Nanoscale.

Supplementary Information

Cyclic Chlorine Trap-Doping for Transparent, Conductive, Thermally Stable and Damage-Free Graphene

Viet Phuong Pham,[†,§] Kyong Nam Kim,[‡,§] Min Hwan Jeon,[†] Ki Seok Kim,[‡] and Geun Young Yeom[†,‡,*]

[†] SKKU Advanced Institute of Nano Technology (SAINT), Sungkyunkwan University (SKKU), Suwon, Gyeonggi-do 440-746, Republic of Korea.

[‡] School of Advanced Materials Science and Engineering, Sungkyunkwan University (SKKU), Suwon, Gyeonggi-do 440-746, Republic of Korea.

[§] These authors contributed equally to this work.

*Address correspondence to gyyeom@skku.edu

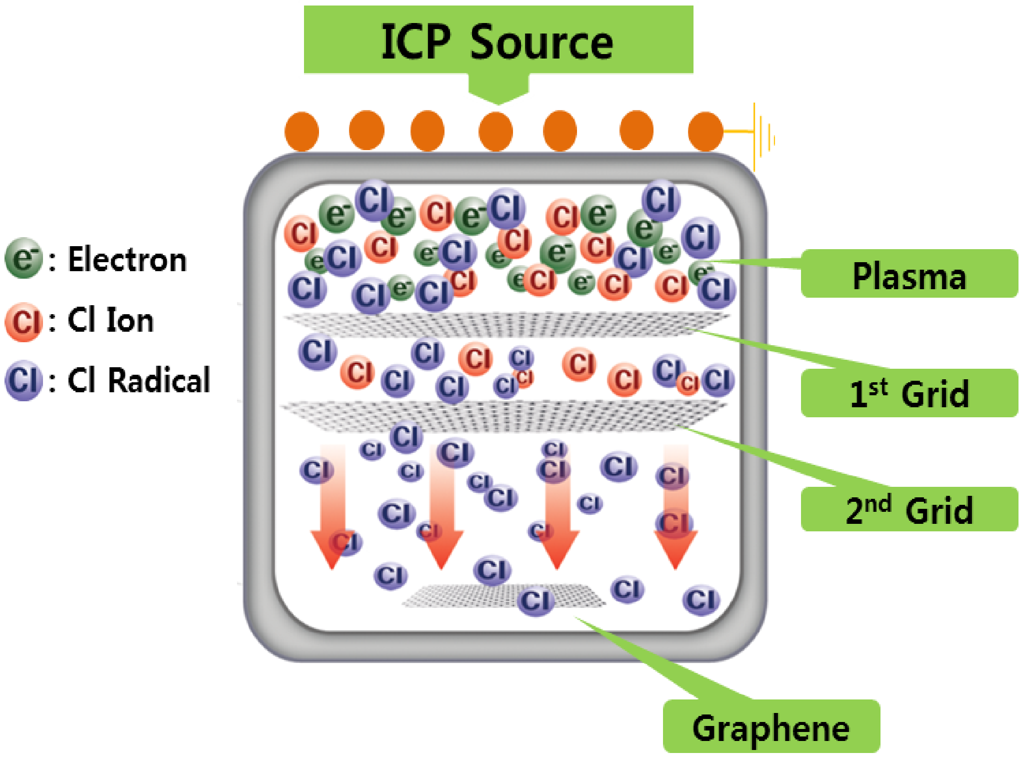

Figure S1. Schematic diagram of a chlorine plasma system with a double-mesh grid used in the cyclic low energy chlorine radical doping.

The chlorine doping system used in the experiment is similar to a conventional inductively coupled plasma (ICP) system. The ICP source composed of a Cu antenna and a dielectric plate was located on the top of the chamber to generate the ICP in the processing chamber. The inside diameter of the processing chamber was 32cm and the size of the substrate holder was 16cm diameter. To generate Cl_2 plasma, 60sccm Cl_2 and 10mTorr of operating pressure were used. As the rf power to the ICP source, 20~300W 13.56MHz ICP power was used. The graphene substrate was inserted in the processing chamber using a loadlock system without breaking the vacuum and the substrate was cooled at about 15℃ with a chiller. Compared to the conventional ICP source, the ICP used in this experiment is equipped with a dual mesh grid in the chamber between the ICP source and the substrate. By locating a dual-mesh grid, the plasma is confined between the ICP source and the substrate and the most of energetic ions in the plasma are also blocked by the mesh grids and only low energy radicals can reach the graphene surface.

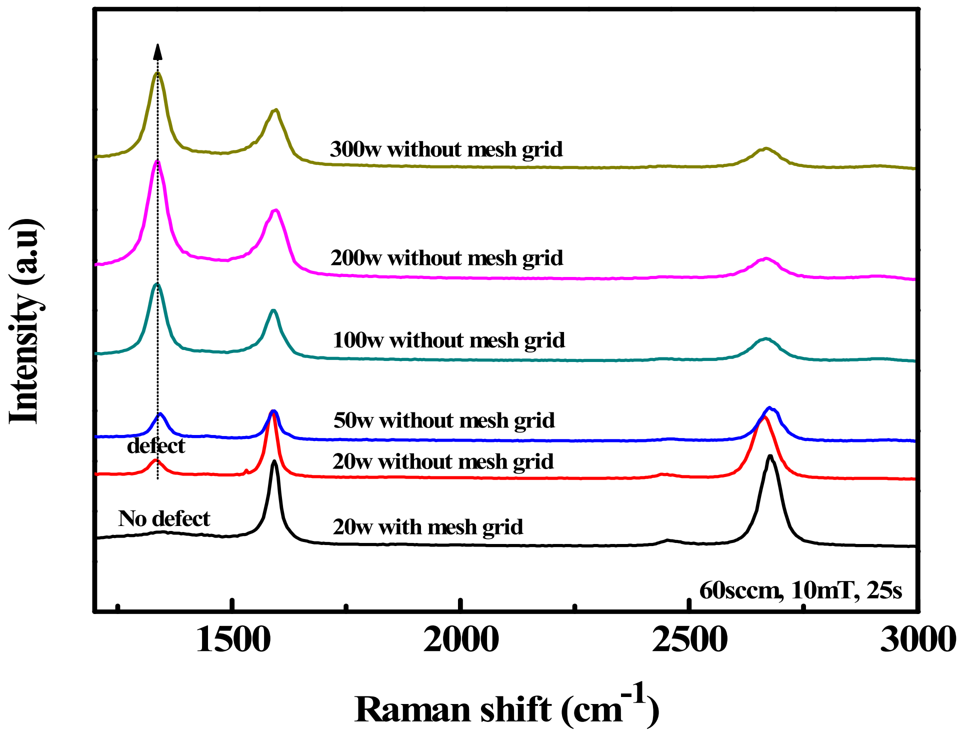

Figure S2. Raman spectra of mono-layer graphene doped by low energy chlorine radicals in a chlorine ICP with / without a double mesh-grid system.

Figure S2 shows the Raman shift of mono-layer graphene measured as a function of rf power to the ICP source in Figure S1. For 20W of rf power, the ICP source was operated with and without a dual-mesh grid between the ICP source and the substrate. 60 sccm Cl_2 and 10mTorr of operating pressure were used. The graphene was treated for 25s. As shown in Figure S2, the use of higher ICP power increased the graphene damage after the chlorine doping by increasing the D peak intensity at 1340 cm^{-1} and by decreasing both the G peak intensity at 1580 cm^{-1} and the 2D peak at 2700 cm^{-1} due to the chlorine ion bombardment. However, with the mesh grid, due to the blocking the most of energetic ions to the substrate while passing the low energy chlorine radicals to the substrate, the chlorine doped graphene showed significantly lower D peak intensity and higher G/2D peak intensities compared to the graphene doped without the mesh grid.

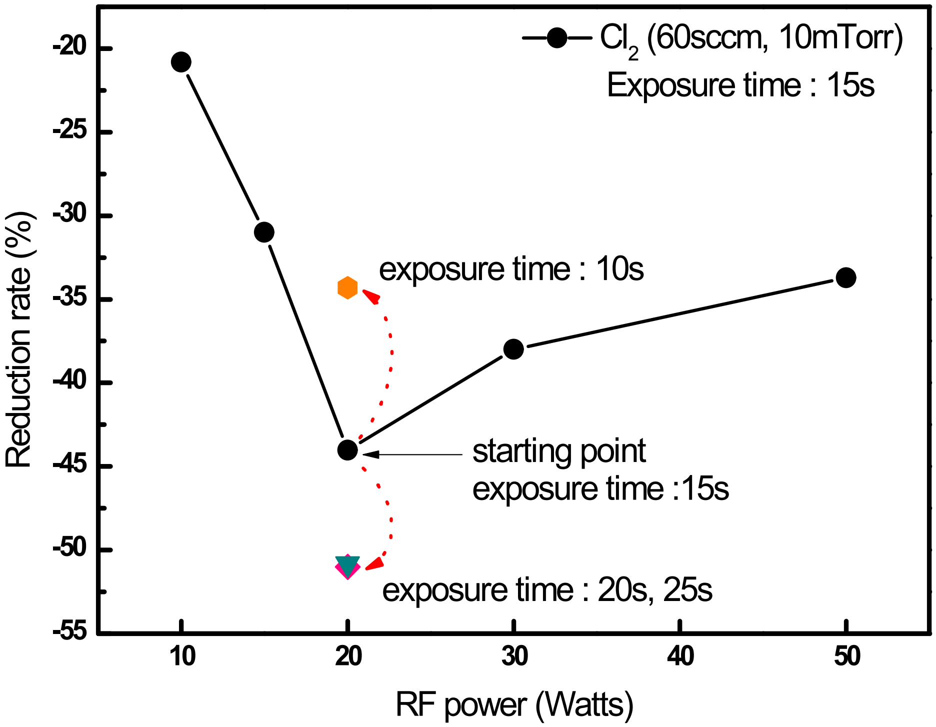

Figure S3. Reduction rate of mono-layer graphene sheet resistance after the chlorine radical doping measured as functions of rf power and exposure time.

Figure S3 shows the sheet resistance change measured as a function of rf power to the ICP source with the double-mesh grid in Figure S1. 10mTorr of the operating pressure was maintained by flowing 60sccm of Cl_2 to the chamber. The plasma exposure time was 15 sec. As shown, the sheet resistance of the mono-layer graphene was decreased with increasing rf power up to 20W of rf power, however, the further increase of rf power increased the sheet resistance. The increase of rf power increases the chlorine radical flux to the substrate by increasing dissociation rate of chlorine gas, however, the increase of rf power also tends to increase the energy of chlorine ions bombarding the substrate even with the mesh grids between ICP source and substrate. The energy of chlorine ions bombarding the substrate should be lower than the sp^2 C-C binding energy of graphene not to damage the graphene surface during the doping. 20W of rf power which showed the lowest sheet resistance in the study is believed to be related to the doping of chlorine with the threshold energy of chlorine ions bombarding the substrate which does not break the sp^2 C-C bonding of the graphene. Also, as shown, while keeping the rf power at 20W, the decrease of plasma exposure time increased the sheet resistance due to the lower doping concentration on the graphene surface, however, when the exposure time was increased more than 20 s, the doping effect is saturated and the sheet resistance was remained similar at the lowest sheet resistance.

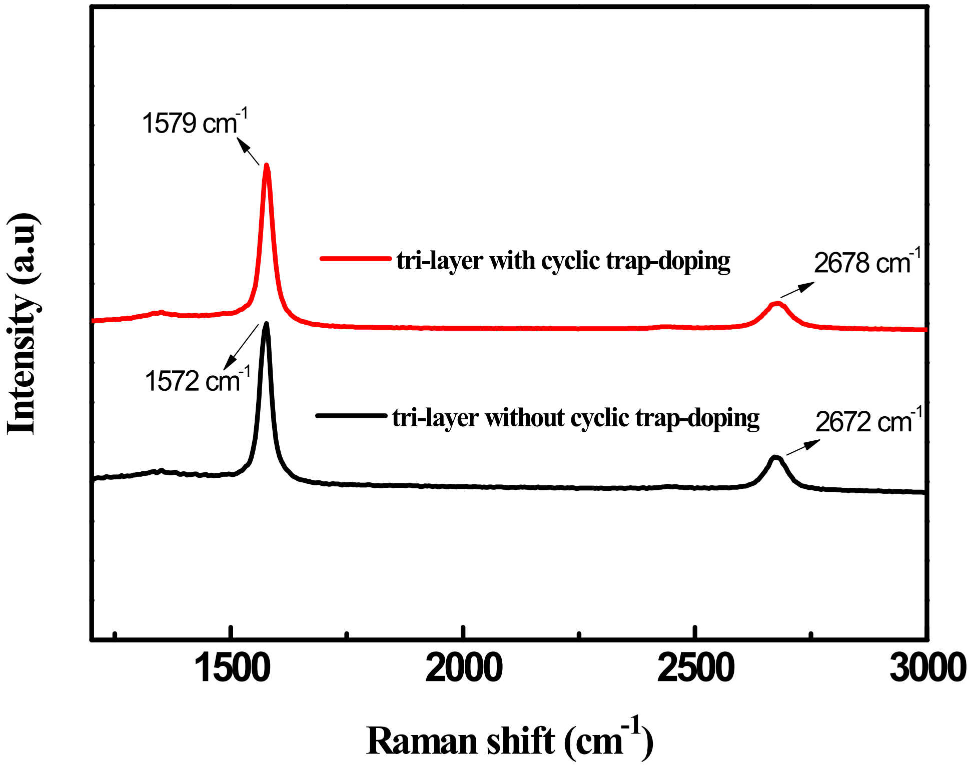

Figure S4. Raman spectra of tri-layer graphene with/without cyclic trap-doping using low energy chlorine radical.

Figure S4 shows the Raman spectra of tri-layer graphene with/without cyclic trap-doping using low energy chlorine radical. As shown in the figure, after the cyclic chlorine trap-doping, the tri-layer graphene did not show any increase of D peak similar to the low energy chlorine doped mono-layer graphene indicating no damage to the graphene layer. In addition, similar to the doped mono-layer graphene, the blue shift of G and 2D peak was also observed indicating doping of graphene.

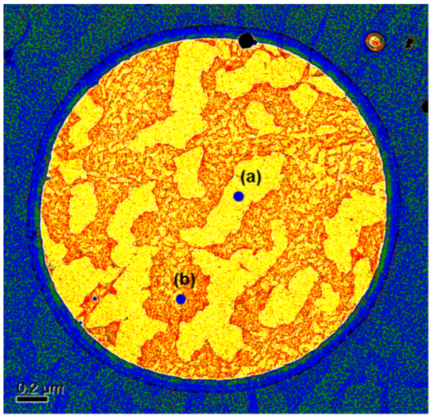

Element	Location	
	Atomic % (a)	Atomic % (b)
C	99	96.23
O	0.88	3.37
Cl	0	0.19
Fe	0.12	0.21

Figure S5. Composition analysis of the bi-layer graphene after the chlorine trap doping process using the micro-EDS in TEM.

Figure S5 shows the micro-EDS data of the bi-layer graphene observed after the chlorine trap doping. Micro-EDS data were taken on the background area (a) and the brown colored area (b) as shown in the figure. As shown on the right side of the figure, a higher chlorine atomic percentage on the brown colored area (b) was observed compared to the background area (a) indicating the existence of chlorine atoms on the brown colored area. The atomic percent of Cl was slightly changed depending on the measured location in TEM due to the irregular distribution of Cl between the graphene layers, however, the brown colored area always showed higher chlorine atomic percentages.

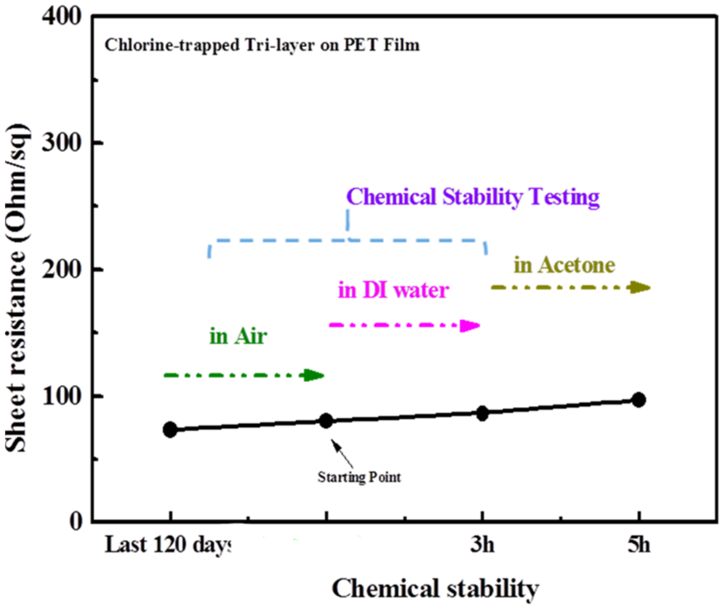

Figure S6. The sheet resistance of chlorine-trapped tri-layer graphene on PET film graphene after exposure to air environment for 120 days after fabrication of the doped graphene on PET film, followed by DI water dipping for three hours, and followed by Aceton cleaning for two hours.

Sheet resistance of the chlorine-trapped tri-layer graphene on PET film graphene measured after the air exposure for 120 days was similar to that measured just after the fabrication. Also, it was not significantly increased even after DI water cleaning for three hours and, followed by Aceton cleaning for two hours. Therefore, the doped graphene investigated in this study was very chemically stable.